Solution-Processed Nanostructured Benzoporphyrin with Polycarbonate Binder for Photovoltaics

Sung-Yu Ku, Christopher D. Liman, Justin E. Cochran, Michael F. Toney, Michael L. Chabinyc, and Craig J. Hawker**

Organic photovoltaics (OPV) based on bulk heterojunctions (BHJs) have efficiencies above 7%[1,2] and can be processed from solution at potentially low cost.[3] BHJs comprise a blend of an electron donor and an electron acceptor in a phase separated morphology that provides a large interfacial area for photogeneration of electron-hole pairs.[4] The highest performance OPVs currently comprise blends of semiconducting polymers and fullerenes, such as [6,6]-phenyl-C_{61}-butyric acid methyl ester (PCBM).[4] Despite their performance in BHJs, semiconducting polymers often take many complicated steps to synthesize and may be difficult to purify.[5,6] Replacing the polymer donor with a small molecule donor is attractive because small molecules have well defined molecular structures, exact molecular weights, and high purity.[7,8]

Solution-processed small molecule BHJ solar cells with efficiencies of 5.2% can be made with blends of (29*H*,31*H*-tetrabenzo[*b*,*g*,*l*,*q*]porphine), BP, and fullerene.[9–11] Although BP is poorly soluble in organic solvents, solution coating is enabled by a soluble precursor (1,4:8,11:15,18:22,25-tetraethano-29*H*,31*H*-tetrabenzo[*b*,*g*,*l*,*q*]porphine), CP (**Figure 1**a) that undergoes a series of retro-Diels Alder reactions on heating to form BP. The detailed mechanism of film formation during thermal conversion is not well understood. BP is attractive as a donor in OPVs because it has an absorption edge near 720 nm and its insolubility allows it to be used in multilayered structures, for example to form an electron blocking layer at the hole extracting electrode.

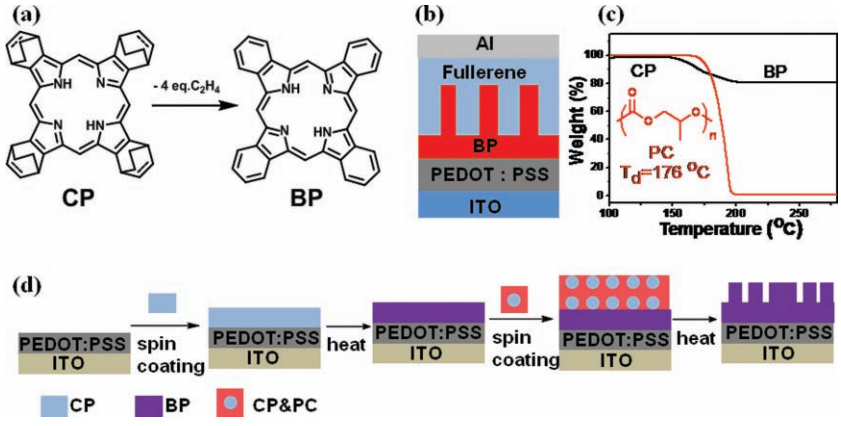

Figure 1. (a) Chemical transformation of BP precursor (CP) to benzoporphyrin (BP) during annealing; (b) standard BP OPV device; (c) TGA analysis of PC and CP; (d) schematic of processing method used to form films of BP for morphology analysis.

One of the barriers to the use of small molecules in BHJs is that they can be difficult to process from solution over large areas. Commercial large area solution-processed solar cells are likely to be fabricated by methods such as inkjet printing[12] and slot or blade coating[13] where control of the viscosity of dilute solutions of small molecules is necessary.[14,15] One method to modify the viscosity of a solution of small molecules is the addition of a polymeric binder that can be removed after deposition. While the control over viscosity by a binder is beneficial, the challenge is that it cannot diminish the electronic properties of the original materials after removal.

In this work, we demonstrate a method to fabricate solution-processed small molecule BHJ solar cells of BP with the aid of a sacrificial thermally degradable binder, poly(propylene carbonate) (PC). We examine the morphological changes in films of BP formed using PC binders through a combination of grazing incidence x-ray scattering (GIWAXS) and scanning electron microscopy (SEM). These studies show that use of PC does not significantly degrade the electronic properties of BP and also helps to form nanostructured film morphologies beneficial to OPVs.

Poly(propylene carbonate) (PC) (Figure 1c), derived from carbon dioxide and propylene oxide, has attracted practical interest with respect to CO_2 fixation and biodegradability.[16] The carbonate linkage in the backbone of PC results in a relatively low thermal decomposition temperature (T_d), potentially limiting its practical applications as a standalone material. However, this low T_d, coupled with decomposition to volatile small molecules, can be exploited in the design of processes involving sacrificial polymer templates.[17,18]

S.-Y. Ku,[†] C. D. Liman,[†] Prof. M. L. Chabinyc, Prof. C. J. Hawker
Materials Research Laboratory
Materials Department
Mitsubishi Chemical Center for Advanced Materials
University of California Santa Barbara
Santa Barbara, CA 93106, USA
E-mail: hawker@mrl.ucsb.edu; mchabinyc@engineering.ucsb.edu
J. E. Cochran
Department of Chemistry and Biochemistry
University of California Santa Barbara
Santa Barbara CA 93106, USA
M. F. Toney
Stanford Synchrotron Radiation Laboratory
Stanford, CA 94305, USA
[†] Dr. S.-Y. Ku and C. D. Liman contributed equally to this work.

DOI: 10.1002/adma.201100028

The incorporation of PC binder into the CP solution increases the viscosity of the solution and improves processability for large area fabrication. To evaluate the range of change in viscosity, solutions of small molecules with and without the PC binder were prepared. The solution with the binder comprised a 2.0 wt% blend of CP and PC (0.6:1.4 weight ratio) in a chloroform:chlorobenzene mixture (1:2 weight ratio). To compare this blend with the solution used to make the BHJ layer in the literature, a solution of small molecules was prepared comprising CP and a fullerene derivative instead of PC. At 25 °C, the viscosity of the control solution of small molecules, 0.8 cP, is not much greater than the viscosity of the solvent mixture (~0.7 cP). However, the viscosity of the solution with the PC binder increases to 1.6 cP. While the increase in viscosity at these low loading levels is modest, such changes are known to have significant impact on coating using inkjet printing where solutions with viscosity in the range of 1–10 cP are desirable.[15,19]–[21] The viscosity may be further increased if necessary for other printing methods, such as screen printing, by using higher concentrations of the binder. In this initial study, we have chosen to work with the lower range of PC loading amenable to inkjet or gravure printing.

To test the influence of the binder on electronic properties, we used the PC binder to form simple films and photovoltaic devices in a modified version of the route that has been used to fabricate OPV devices with BP. The best photovoltaic devices with BP have been obtained using a *p-i-n* structure. In this nomenclature, *p* refers to an electron-blocking layer of pure BP, *i* refers to a blend of BP:fullerene, and *n* refers to a hole-blocking layer of pure fullerene. A BHJ photovoltaic cell with BP is made in a multi-step process. First, the soluble precursor CP is spin-coated onto a glass/ITO/PEDOT:PSS anode, then heated at 180 °C to convert it to the highly insoluble, crystalline BP donor with the release of ethylene (Figure 1a) to create the *p*-layer. Then a blend of CP and a soluble fullerene is spin-coated on top and thermally converted to create the *i*-layer. This heating and conversion process does not cause the fullerene to react or degrade, but does cause it to crystallize.[9–11] Finally, the soluble fullerene is spin-coated on top to create the *n*-layer, and an Al cathode was thermally evaporated (Figure 1b). Matsuo et al. has demonstrated that photovoltaic cells formed with a BHJ of BP and SIMEF (1,4-bis(dimethylphenylsilylmethyl[60]fullerene) with a 2,9-bis(naphthalen-2yl)-4,7-diphenyl-1,10-phenanthroline buffer layer between the *n* layer and Al electrode can achieve a power-conversion efficiency of 5.2%.[11] Here, we modify this process by using a PC binder in the coating of the CP precursor layers.

A critical aspect of the sacrificial polymer binder strategy is the effect of the PC binder on the morphology of BP films. To assess this effect, the donor component of the *i*-layer and also the *p*-layer were fabricated through the CP:PC route. To make the standard *p*-layer, the CP solution is first spin-coated on a glass/ITO/PEDOT:PSS substrate for devices (or a Si/PEDOT:PSS substrate for morphological studies) and is thermally converted to the donor BP at 180 °C (Figure 1d). In the second step, a homogeneous mixture of degradable PC binder (0.25 wt%) and CP (0.75wt%) in a co-solvent of chloroform and either chlorobenzene or 2-chloroethanol is spin-coated to form the CP:PC layer. The conversion of CP to BP occurs at 180 °C which is the same temperature that PC begins to decompose. Complete removal of PC requires heating to 200 °C. Therefore, the samples were heated first to 180 °C to convert the soluble CP precursor to insoluble BP, and then to 200 °C to remove residual PC binder, resulting in a nanostructured BP layer. The resulting structure is PEDOT:PSS/BP/BP′, where BP′ denotes a layer made through the CP:PC route. The gaps in this film can be backfilled with a fullerene to form the *i*-layer. A second set of samples was fabricated containing only the *p*-layer made through the CP:PC route to investigate the effect of using the CP:PC route on top of PEDOT:PSS rather than BP as well. The procedure used was the same as that of the *i*-layer, but without the underlying BP layer, resulting in a PEDOT:PSS/BP′ structure.

Top-down view and cross-section SEM images were used to observe the resulting morphology and nanostructure of the films. Grazing incidence wide angle X-ray scattering (GIWAXS) with 2-dimensional detection was used to study the crystal structure and texture in the BP films. In the bulk, BP crystallizes in a monoclinic unit cell with the $P2_1/n$ space group.[22] Through GIWAXS, it was found that fully annealed PEDOT:PSS/BP/BP′ films formed by the CP:PC route as well as PEDOT:PSS/BP films formed by the standard route have this same crystal structure (see Supporting Information, S.I.). Significantly, GIWAXS characterization was also performed on these films while annealing in situ (see S.I.), and it was shown that the sacrificial binder does not affect the final crystal structure. The texture of these films, i.e. the distribution of orientations of the crystallite domains, was also examined. First, the texture of PEDOT:PSS/BP/BP′ films made through the CP:PC route was compared to that of PEDOT:PSS/BP films made through the standard route. The intensities of the diffraction peaks with respect to angle from the vertical axis (β) in 2-D GIWAXS plots were nearly the same for both types of films (**Figure 2**c and Figure 2f).

While it was shown that addition of the PC binder does not impact molecular scale ordering in BP′ films, it does affect the large-scale morphology. The morphological influence of the PC binder on the PEDOT:PSS/BP/BP′ film is to create a textured nanostructure that is appropriate for BHJ solar cells. Through SEM, it was found that the vast majority of the surface consists of rectangular BP columns (ca. diameter of 50–100 nm and height of 100–150 nm) (Figure 2d and 2e). In contrast, a film of PEDOT:PSS/BP formed by the standard route revealed two types of crystal shapes, consisting of large flat regions in the majority and smaller vertical domains in the minority (Figure 2a and 2b), with few gaps in the film. Films of PEDOT:PSS/BP/BP also show a similar morphology, but with a slightly more ordered and uniform packing of the grains (see S.I.). The difference in morphology does not affect crystallographic texture as seen in GIWAXS; the texture is a result of the orientation of crystallites, which may not depend on the possible gaps between them. It is conjectured that the reason for the difference in morphology is that during the annealing process for a neat BP film formed by the standard route, CP transforms to BP with 20% weight loss by releasing 4 equivalents of ethylene. In direct contrast, CP:PC films undergo ca. 40% weight loss due to the additional presence of PC binder and the released small molecule mixture consisting of ethylene, CO_2 and acetone. The weight loss of CP:PC films not only results in thinner films, but

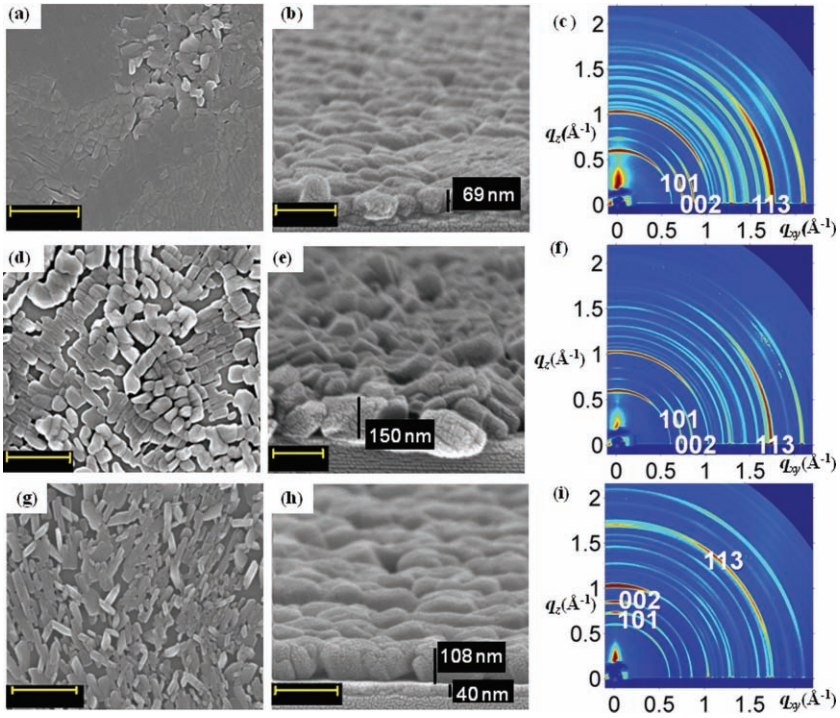

Figure 2. Sample A (PEDOT:PSS/BP), sample B (PEDOT:PSS/BP/BP′) and sample C (PEDOT:PSS/BP′); scale bar in top view image is 1 μm; scale bar in cross-section is 200 nm; film thicknesses obtained by SEM are approximate. (a) top view SEM of sample A; (b) cross-section SEM of sample A; (c) 2-D GIWAXS of sample A; (d) top view SEM of sample B; (e) cross-section SEM of sample B; (f) 2-D GIWAXS of sample B; (g) top view SEM of sample C; (h) cross-section of sample C; (i) 2-D GIWAXS of sample C.

also disrupts and changes the morphology of the BP crystals, resulting in the desired ordered polycrystalline BP′ with nanoscale (50–100 nm) gaps between each crystallite. When the gaps between the crystallites are filled with acceptor material, the morphology forms the BHJ *i*-layer.

We also examined the use of CP:PC solutions to form the *p*-layer of the photovoltaic devices. PEDOT:PSS/BP′ films were not advantageous for the *p*-layer relative to films formed without polycarbonate. They have a less desirable crystal texture due to a wider range of crystallite orientations and morphology due to gaps in the film to the underlying PEDOT:PSS layer. After annealing, the integration of 2-D GIWAXS patterns of these films over all β showed crystal structures for the BP′ in these films to be the same as that of the previously mentioned films (see S.I.). However, the intensities of the diffraction peaks with respect to β show that the texture is different (Figure 2i and S.I.). In PEDOT:PSS/BP′ films, the (101) and (002) rings are most intense on the q_z axis of the figure (defined as $\beta = 0°$), indicating that most crystallite orientations have these planes parallel to the substrate. In comparison, for PEDOT:PSS/BP and PEDOT:PSS/BP/BP′ films, these rings are most intense on the q_{xy} axis, indicating that these planes are perpendicular to the substrate. Because the (101) and (002) planes both contain the *b*-axis of the unit cell [010], a large fraction of crystallites in the latter two films have the *b*-axis is oriented perpendicular to the substrate. This texture is beneficial for charge transport in solar cells because it has been suggested that the *b*-axis of BP has better hole mobility than the *a*- and *c*-axes due to π-π stacking.[23] The morphology of PEDOT:PSS/BP′ films comprises large rectangular columns of BP approximately 300 nm in width and 100 nm in height as shown in Figure 2g and 2h. In addition to the GIWAXS data, this also suggests that the long direction of the crystallites parallel to the surface is the *b*-axis. This texture may be beneficial for charge transport in thin film transistors (TFTs), but the films are currently too rough to produce TFTs at readily obtainable channel lengths. Overall, the data show that for benzoporphyrin films made through the CP:PC route, the morphology and crystal texture is affected by interactions with the substrate. The more continuous base layer of PEDOT:PSS/BP in BP′ samples results in much better crystal coverage as well as smaller crystals useful for BHJ devices.

Films utilizing the BHJ morphology created as a result of the PC binder can be used to make effective solar cells that are compatible with large area fabrication methods. OPVs made with PEDOT:PSS/BP/BP′ films through the CP:PC route were fabricated and compared with devices made through the standard route (**Figure 3** and **Table 1**). To test the hypothesis that fullerene can be added to the nanostructured BP′ layer to produce an *i*-layer, PCBNB ([6,6]-phenyl-C_{61}-butyric acid n-butyl ester) was spin-coated on top of PEDOT:PSS/BP/BP′ samples and annealed, and finally thermal evaporation was used to deposit an aluminum electrode, resulting in the *p-i* PEDOT:PSS/BP/BP′:PCBNB/Al structure. In another set of devices, the BP′ layer was treated as an additional *p*-layer and therefore a standard *i*-layer of CP:PCBNB was spin coated on top and thermally converted, and finally aluminum was deposited, resulting in the *p-i* PEDOT:PSS/BP/BP′/BP:PCBNB/Al structure. Samples spun from two different co-solvent blends were also tested. These two types of devices were compared to the standard *p-i* and *p-i-n* control BP-based solar cells, made by starting with PEDOT:PSS/BP followed by spin-coating an *i*-layer of CP:PCBNB on top and thermally converting, optionally spin-coating an *n*-layer of PCBNB, and depositing aluminum.

Measurements of solar power conversion efficiency demonstrate that the CP:PC route can be used to make OPV devices

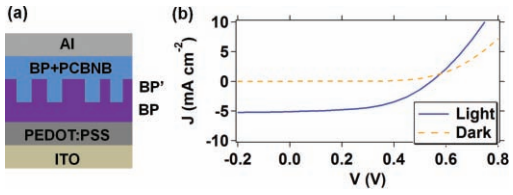

Figure 3. (a) BP OPV device made through the CP:PC route; (b) *J–V* curve of device type PEDOT:PSS/BP/BP′/BP:PCBNB/Al (chlorobenzene:chloroform) in Table 1, tested under 1 sun at AM 1.5 simulated conditions. *J–V* curves of other devices are in Figure SI-3.

Table 1. OPV device data (average of five devices).

Type	Device Structure	Route	V_{oc} [V]	J_{sc} [mA/cm^2]	FF	EQE (%)
p-i	PEDOT:PSS/BP/BP′:PCBNB/Al	CP:PC[a)]	0.57	4.33	0.46	1.12
p-i	PEDOT:PSS/BP/BP′:PCBNB/Al	CP:PC[b)]	0.54	5.15	0.48	1.35
p-i	PEDOT:PSS/BP/BP′/BP:PCBNB/Al	CP:PC[a)]	0.60	4.67	0.42	1.19
p-i	PEDOT:PSS/BP/BP′/BP:PCBNB/Al	CP:PC[b)]	0.55	5.12	0.51	1.43
p-i	PEDOT:PSS/BP/BP:PCBNB/Al	Standard	0.58	5.48	0.49	1.54
p-i-n	PEDOT:PSS/BP/BP:PCBNB/PCBNB/Al	Standard	0.41	5.45	0.60	1.34

[a)] The CP:PC solution was prepared with 2:1 by volume of chloroform:2-chloroethanol; [b)] The CP:PC solution was prepared with 2:1 by volume of chlorobenzene:chloroform.

without sacrificing performance). The efficiencies (1.35%) of *p-i* devices with an *i*-layer of BP′:PCBNB were only slightly below those of the *p-i* control devices made by the standard route (1.54%). By fitting the current-voltage curves of these devices with the Hecht expression for charge extraction,[24] it was determined that they had similar mobility-lifetime ($\mu\tau$) products of 5.5×10^{-10} cm^2/V and 5.0×10^{-10} cm^2/V respectively suggesting similar electronic properties in both cases. Devices in which CP:PC was spun from chlorobenzene:chloroform (CB:CL) were more efficient than devices in which CP:PC was spun from chloroform:2-chloroethanol (CL:CE) demonstrating that the efficiency is sensitive to the solvent used for casting. However, the morphology of the two observed by SEM was similar (see S.I.) Besides viscosity control, an advantage of using this route to create an *i*-layer is the increased flexibility when adding the fullerene derivative or other acceptor. It does not require the acceptor to be annealed, increasing the potential range of solvents for the acceptor, and causes the BHJ feature size to be independent of the choice of acceptor. Similar morphologies can be formed with different acceptors simplifying the evaluation of new materials.

The strategy of treating BP′ as an additional *p*-layer and adding a standard *i*-layer of BP:PCBNB to form a PEDOT:PSS/BP/BP′/BP:PCBNB/Al device was also examined. These devices had similar efficiency (1.43%) to PEDOT:PSS/BP/BP′:PCBNB/Al devices where BP′:PCBNB was the *i*-layer (1.35%). Through SEM, it was found that these devices exhibited a BHJ that contained both a larger and a smaller feature size (~100 nm from BP′ and 20 nm from BP:PCBNB). The morphology consists of smaller columnar nanostructures due to the BP:PCBNB, on top of larger rectangular crystallites due to the BP′ (see S.I.). Interestingly, when an *n*-layer consisting of PCBNB is added to the control *p-i* devices to form *p-i-n* devices, the efficiency actually goes down (1.54% to 1.34%). Because the total device thickness remains the same and the short circuit current remains the same, this difference is due mainly to the difference in the open circuit voltage, V_{oc}. Examination of the dark current shows that these devices have larger forward bias currents than the others causing a reduction in V_{oc}. The origin of the differences likely lies in the energetic line-up at the aluminum electrode, and is a topic for future work.

It is important to note that the insulating PC binder could easily diminish device efficiency and hole transport properties if it did not completely degrade. However, the J_{sc} of devices made by the CP:PC route reached 5.1 mA/cm^2, which is comparable to the J_{sc} of devices made by the standard route. This observation suggests that after the annealing process and deposition of the fullerene that there is little or no residue from the PC binder in the BP′ film to impede charge carrier generation.

In conclusion, this work has shown that a thermally degradable binder strategy in processing solar cells based on small molecule donors and fullerene acceptors results in improved process control without sacrificing efficiency. A poly(propylene carbonate) binder allowed control of the solution viscosity without harming optoelectronic performance. Significantly the use of PC does not change the crystal structure or texturing of BP relative to the neat films, but it does result in increased nanoscale texturing and surface area that is desirable for subsequent deposition of a fullerene-based acceptor. Besides controlling viscosity, another advantage of using a decomposable binder such as PC to form a BHJ is increased flexibility in the choice and processing of the acceptor. One drawback of this method is that it currently requires an underlying BP layer fabricated from a lower viscosity solution, to alleviate roughness and gaps in the film. But the use of other decomposable polymers such as poly(acetaldehyde) and the optimization of polymer:BP phase separation could eliminate this requirement. Most importantly, photovoltaic devices with this BHJ exhibit comparable performance to the previously used method of simply mixing the BP and PCBNB suggesting that the decomposable binder does not degrade photovoltaic power conversion efficiency.

Experimental Section

Solution Preparation: CP (1,4:8,11:15,18:22,25-tetraethano-29*H*,31*H*-tetrabenzo[*b*,*g*,*l*,*q*]porphine, i.e. bicycloporphyrin) and PCBNB ([6,6]-phenyl-C_{61}-butyric acid n-butyl ester) were obtained from Mitsubishi Chemical. PC (poly(propylene carbonate)) was obtained from Novomer. TGA was conducted on the PC and BP precursor. Solutions of 7 mg/mL CP in a co-solvent of 2:1 chlorobenzene:chloroform, as well as 2:1 chloroform:2-chloroethanol, were prepared. Solutions of 7.5 mg/mL CP and 2.5 mg/mL PC in both of these co-solvents were also prepared. Solutions of 6 mg/mL CP and 14 mg/mL PCBNB in 1:1 chlorobenzene:chloroform were prepared. Finally, solutions of 12 mg/mL PCBNB in toluene were prepared. Viscosity measurements were conducted with an RE-80L viscometer (TOKI SANGYO CO., LTD.)

Film Preparation: Glass/ITO (indium tin oxide) and Si substrates were sonicated in acetone, soap and DI water, DI water, and isopropanol for 20 minutes each. PEDOT:PSS (poly(3,4-ethylenedioxythiophene) poly(styrenesulfonate)), brand name Clevios PH) was obtained

from H.C. Starck and spin coated onto glass/ITO substrates at 4500 rpm to form films about 40 nm thick. CP films (about 20 nm thick from chlorobenzene:chloroform and about 40 nm thick from chloroform:chloroethanol) were spin-coated in a glovebox at 1500 rpm speed onto Si and glass/ITO/PEDOT:PSS substrates. The films were annealed in a glovebox for 20 min at 180 °C to thermally decompose the CP to BP (29*H*,31*H*-tetrabenzo[*b*,*g*,*l*,*q*]porphin, i.e. benzoporphyrin). CP:PCBNB films about 110 nm thick were spin-coated at 1500 rpm speed and annealed for 20 min at 180 °C. CP:PC films about 130 nm thick were spin-coated at 1500 rpm speed and 500 acceleration and annealed for 20 min at 180 °C, then for 20 min at 200 °C, to transform CP to BP′ and thermally decompose the PC without residue. PCBNB films were spin-coated at 1500 or 3000 rpm speed and dried for 10 min at 65 °C.

Device Fabrication and Testing: On the glass/ITO/PEDOT:PSS/active layer samples, the PEDOT:PSS and active layer were scraped off on one side to allow Al to deposit on the ITO electrode. 90 nm of Al was thermally evaporated using a mask, creating 5 top contact pixels and a bottom contact to the ITO. The devices were placed in a solar simulator in a glovebox and tested under 1 sun and in the dark to obtain *J*–*V* curves.

Sample Characterization: Film thicknesses were measured by profilometry. Absorption spectroscopy was conducted on samples with glass substrates at various annealing times. Top-down and cross-section SEM were conducted on samples with Si substrates using an FEI XL30 Sirion FEG microscope. 2D grazing incidence wide angle X-ray scattering (GIWAXS) on the 11–3 beamline at the Stanford Synchrotron Radiation Lightsource (SSRL) was conducted on samples with Si substrates. The WxDiff program and the GIXD Analysis Routine for Igor Pro were used to analyze GIWAXS data.

Supporting Information

Supporting Information is available from the Wiley Online Library or from the author.

Acknowledgements

We thank M. Guide, N. Treat, M. Burkhardt, J. Heo, and M. Dimitriou for their insights, N. Eisenmenger and C. Shuttle for assistance with OPV testing, and Eric Verploegen for assistance with the in-situ annealing. We thank the Mitsubishi Chemical Group Science and Technology Research Center, Inc. for sharing their insights and provision of CP and analytical data. Software for analyzing GIWAXS data was written by Stefan Mannsfeld (SSRL) and R. Joseph Kline (NIST). Portions of this research were carried out at the Stanford Synchrotron Radiation Lightsource, a national user facility operated by Stanford University on behalf of the U.S. Department of Energy, Office of Basic Energy Sciences. This work was supported by the NSF SOLAR program (CHE-1035292), Mitsubsihi Chemicals Center for Advanced Materials and the UCSB MRSEC Program under NSF award DMR05–20415. This article is part of the Special Issue on Materials Research at the University of California, Santa Barbara.

Received: January 5, 2011
Revised: March 8, 2011
Published online: April 26, 2011

[1] Y. Liang, Y. Wu, D. Feng, S.-T. Tsai, H.-J. Son, G. Li, L. Yu, *J. Am. Chem. Soc.* **2009**, *131*, 56.
[2] Y. Liang, Z. Xu, J. Xia, S.-T. Tsai, Y. Wu, G. Li, C. Ray, L. Yu, *Adv. Mater.* **2010**, *22*, E135.
[3] C. J. Brabec, N. S. Sariciftci, J. C. Hummelen, *Adv. Funct. Mater.* **2001**, *11*, 15.
[4] G. Dennler, M. C. Scharber, C. J. Brabec, *Adv. Mater.* **2009**, *21*, 1323.
[5] J. E. Anthony, M. Heeney, B. S. Ong, *MRS Bull.* **2008**, *33*, 698.
[6] Y.-J. Cheng, S.-H. Yang, C.-S. Hsu, *Chem. Rev.* **2009**, *109*, 5868.
[7] J. Roncali, *Acc. Chem. Res.* **2009**, *42*, 1719.
[8] G. Wei, R. R. Lunt, K. Sun, S. Wang, M. E. Thompson, S. R. Forrest, *Nano Lett.* **2010**, *10*, 3555.
[9] Y. Sato, T. Niinomi, M. Hashiguchi, Y. Matsuo, E. Nakamura, *Proc. SPIE* **2007**, *6656*, 66560U.
[10] Y. Sato, T. Niinomi, Y. Abe, Y. Matsuo, E. Nakamura, *Proc. SPIE* **2008**, *7052*, 70520J.
[11] Y. Matsuo, Y. Sato, T. Niinomi, I. Soga, H. Tanaka, E. Nakamura, *J. Am. Chem. Soc.* **2009**, *131*, 16048.
[12] M. Singh, H. M. Haverinen, P. Dhagat, G. E. Jabbour, *Adv. Mater.* **2010**, *22*, 673.
[13] Y.-H. Chang, S.-R. Tseng, C.-Y. Chen, H.-F. Meng, E.-C. Chen, S.-F. Horng, C.-S. Hsu, *Org. Electron.* **2009**, *10*, 741.
[14] C. J. Brabec, J. R. Durrant, *MRS Bull.* **2008**, *33*, 670.
[15] F. C. Krebs, *Solar Ener. Mater. Solar Cells* **2009**, *4*, 394.
[16] X. Chen, Z. Shen, Y. Zhang, *Macromolecules* **1991**, *24*, 5305.
[17] J. L. Hedrick, T. Magbitang, E. F. Connor, T. Glauser, W. Volksen, C. J. Hawker, V. Y. Lee, R. D. Miller, *Chem. Eur. J.* **2002**, *8*, 3308.
[18] T. Rajagopalan, B. Lahlouh, J. A. Lubguban, N. Biswas, S. Gangopadhyay, J. Sun, D. H. Huang, S. L. Simon, A. Mallikarjunan, H.-C. Kim, W. Volksen, M. F. Toney, E. Huang, P. M. Rice, E. Delenia, R. D. Miller, *Appl. Phys. Lett.* **2003**, *82*, 4328
[19] B.-J. de Gans, P. C. Duineveld, U. S. Schubert, *Adv. Mater.* **2004**, *16*, 203.
[20] C. N. Hoth, P. Schilinsky, S. A. Choulis, C. J. Brabec, *Nano Lett.* **2008**, *8*, 2806.
[21] J. Perelaer, P. J. Smith, M. M. P. Wijnen, E. Van Den Bosch, R. Eckardt, P. H. J. M. Ketelaars, U. S. Schubert, *Macromol. Chem. Phys.* **2009**, *210*, 387.
[22] S. Aramaki, J. Mizuguchi, *Acta Crystallogr. E* **2003**, *59*, 1556.
[23] N. Noguchi, S. Junwei, H. Asatani, M. Matsuoka, *Cryst. Growth Des.* **2010**, *10*, 1848.
[24] R. A. Street, M. Schoendorf, A. Roy, J. H. Lee, *Phys. Rev. B* **2010**, *81*, 205307.